coatings

MDPI

Article

Osteogenic and Antibacterial Activity of a Plasma-Sprayed CeO_2 Coating on a Titanium (Ti)-Based Dental Implant

Jing Yue [1,†], Zhichun Jin [2,†], Hin Lok Enoch Poon [3,4], Guangwei Shang [1], Haixia Liu [1], Dan Wang [3,4], Shengcai Qi [1], Fubo Chen [1,*] and Yuanzhi Xu [1,*]

1 Department of Stomatology, Shanghai Tenth People's Hospital, Tongji University School of Medicine, Shanghai 200072, China; jingyue624@163.com (J.Y.); gwshang99@yahoo.com (G.S.); 13673530995@163.com (H.L.); dentistqi@163.com (S.Q.)
2 Jiangsu Key Laboratory of Oral Diseases, Affiliated Hospital of Stomatology, Nanjing Medical University, Nanjing 211166, China; jinzhichun@126.com
3 Institute for Tissue Engineering and Regenerative Medicine, The Chinese University of Hong Kong, Hong Kong 999077, China; enochhlpoon@link.cuhk.edu.hk (H.L.E.P.); wangmd@cuhk.edu.hk (D.W.)
4 School of Biomedical Sciences, Faculty of Medicine, The Chinese University of Hong Kong, Hong Kong 999077, China
* Correspondence: chenfubo@126.com (F.C.); amyxyz01@hotmail.com (Y.X.); Tel.: +86-02166301722 (F.C.)
† Both contributed equally to this work.

Received: 11 September 2020; Accepted: 9 October 2020; Published: 21 October 2020

Abstract: Peri-implantitis, often induced by oral pathogens, is one of the main reasons for the clinical failure of dental implants. The aim of this study was to investigate the biocompatibility, osteogeneic, and antibacterial properties of a cerium oxide (CeO_2) coating containing high proportions of Ce^{4+} valences on a titanium-based dental implant biomaterial, Ti-6Al-4V. MC3T3-E1 cells or bone marrow stem cells (BMSCs) were seeded onto Ti-6Al-4V disks with or without CeO_2 coating. Compared to the control, the plasma-sprayed CeO_2 coating showed enhanced cell viability based on cell counting kit-8 (CCK-8) and flow cytometry assays. CCK-8, colony-forming unit test (CFU), and live-dead staining illustrated the antibacterial activity of CeO_2 coating. Additionally, CeO_2 coating upregulated the gene expression levels of osteogenic markers *ALP*, *Bsp* and *Ocn*, with a similar increase in protein expression levels of OCN and Smad 1 in both MC3T3-E1 cells and BMSCs. More importantly, the viability and proliferation of *Enterococcus faecalis*, *Prevotella intermedia*, and *Porphyromonas gingivalis* were significantly decreased on the CeO_2-coated Ti-6Al-4V surfaces compared to non-treated Ti-6Al-4V. In conclusion, the plasma-sprayed CeO_2 coating on the surface of Ti-6Al-4V exhibited strong biocompatibility, antibacterial, and osteogenic characteristics, with potential for usage in coated dental implant biomaterials for prevention of peri-implantitis.

Keywords: CeO_2 coating; antibacterial activity; biocompatibility; osteogenic differentiation

1. Introduction

Dental implantation, an indispensable and established dental therapy, is a widely adopted replacement for missing teeth in various clinical situations. Nevertheless, evidence from recent decades has shown an increasing presence of peri-implantitis associated with the use of dental implants [1]. Peri-implant mucositis was detected in approximately 60.2% of implants in 73.1% of patients, while peri-implantitis affected 12% of implants in 15.4% of patients [2]; The resultant inflammatory processes damage both soft and hard tissues surrounding the implants, which were attributed as a major cause of dental implant failures [3]. The occurrence of peri-implantitis is

primarily traced to the presence of gram-negative anaerobic microflora [4], of which the species *Porphyromonas gingivalis (P.g.)* and *Prevotella intermedia* (*P.i.*) are the dominant cause of periodontitis and peri-implantitis [5]. In addition, traces of *Enterococcus faecalis* (*E.f.*) can be found in the osseous environs of infected implants, indicating its involvement in peri-implantitis [6]. *E.f.* has been pervasive in dental infections and was adopted as a test for abutment seals in dental implant designs [7,8]. Furthermore, *E.f.* is known to tolerate physiologically harsh environments such as high-pH alkaline conditions and nutritional deficiency. Thus, it has been a recurrent challenge for dentists to eliminate *E.f. P.g.* and *P.i.* in peri-implantitis.

Titanium (Ti)-based dental implants are widely employed due to their superior osseointegration properties beneficial to the structural integrity and durability of the implants [9,10], with the titanium alloy Ti-6AL-4V frequently adopted due to its intrinsic mechanical strength and resistance as compared to pure titanium [11]. Due to severe consequences of peri-implantitis brought on the integrity of dental implants, strategies for treatment or prevention of peri-implantitis are an important area of discussion [12]. Much of the published strategies for peri-implantitis therapy focus on treatments similar to those adopted for periodontitis [13–17]. Compared to treatment, prevention is the more important strategy along with appropriate treatment planning, continuous check-up intervals, and professional teeth/implant cleaning [1]. Currently, antibacterial surface coatings on dental implants have attracted great attention due to the ease in applying on dental implant surfaces without impacting its physical properties [18]. Various titanium-based dental implant surfaces can be obtained in different ways, such as machining, acid etching, anodization, plasma spraying, grit blasting, or combination techniques yielding materials with smooth or microroughened surfaces [19]. Thus, ideal surface coatings for dental implants should prevent polymicrobial infection while enabling excellent osseointegration [20]. Plasma-sprayed biocoatings on Ti-6Al-4V, which have a significantly greater bonding strength compared with Ti-6Al-4V substrata, are potential biomaterials for implant applications [21,22]. Previous research has elucidated the osteogenic properties of cerium oxide (CeO_2)-incorporated hydroxyapatite coatings on Ti-6Al-4V [23]. Furthermore, previous work has shown that a higher percentage of Ce^{4+} valence states promoted the osteogenic behaviors of bone marrow stem cells (BMSCs), potentially benefitting its inclusion in dental implant applications [24]. However, the antibacterial of the high percentage of Ce^{4+} in CeO_2 coatings on Ti-6Al-4V implants has yet to be reported in literature.

In this study, a CeO_2 coating with high percentage of Ce4+ valences was applied via plasma spraying technique onto Ti-6Al-4V substrates. The antibacterial effects of CeO_2 on *E.f.*, *P.g.*, and *P.i.* were investigated in vitro via CCK-8, CFU, and live-dead cell staining assays, with flow cytometry performed as further validation of the results. The biocompatibility and osteogenic activity of the CeO_2 coating on both MC3T3-E1 cells and human bone marrow stem cells (BMSCs) was evaluated by CCK-8, real-time PCR, and Western blot.

2. Materials and Methods

The entire study was performed according to informed protocols approved by the Ethics Committee of Shanghai Tenth People's Hospital, Tongji University School of Medicine.

2.1. Preparation and Characterization of the CeO_2 Coating

CeO_2 powder was prepared via a high-temperature solid-state reaction using CeO_2 (A.R., SCRC, China) as the raw material. An atmosphere plasma spraying (APS) system (F4-MB, Sulzer Metco, Switzerland) was applied to fabricate the coating on the Ti-6Al-4V substrate with dimensions of ø 34 mm × 1 mm and ø 10 mm × 1 mm. Detailed preparation of the powders and coating was described in a previous study [25]. Briefly, the plasma spray process used a direct current (DC) electric arc to generate a stream of high temperature ionized plasma gas, which acted as the spraying heat source. The CeO_2 powder was carried in an inert gas stream into the plasma jet where it was heated and propelled towards the Ti alloy substrate. The phase chemical composition of the powder-sprayed coating was measured using an X-ray diffractometer (XRD, D/max 2500 V, Rigiku, Tokyo, Japan)

with Cu Kα radiation. Surface microstructure of the sprayed coating was observed by field emission scanning electron microscopy (FE-SEM, SU8200, Hitachi, Tokyo, Japan). The test samples were dehydrated using alcohol and sputter-coated with gold before the FE-SEM. Additionally, in order to quantify the ratio of Ce^{3+}/Ce^{4+} valence state in the CeO_2 coating, the coating samples were analyzed by X-ray photoelectron spectroscopy (XPS, MICRO-LAB 310F, Thermo Fisher Scientific, Waltham, MA, USA) Al ka X-ray source.

2.2. Cell Biocompatibility and Osteogenic Behaviors of the CeO_2 Coating

2.2.1. Cell Viability Assay

Primary mouse bone marrow-derived mesenchymal stem cells (BMSCs) were isolated from the bone marrow cavity of the tibias of 3-week-old C57BL/6 mice and cultured in BMSC growth medium (α-MEM medium containing 10% FBS, 100 U/mL penicillin and 100 mg/mL streptomycin). Briefly, aspirates were flushed with growth medium and seeded in 10 cm Petri dishes for 3 days. Adherent BMSCs were further cultured and expanded. Passage 3–6 cells were used in experiments.

Cell counting kit-8 (CCK-8; Dojindo Kagaku Co., Kumamoto, Japan) was used to analyze cell viability according to the manufacturer's protocols. BMSCs and MC3T3-E1 cells were used in this section. A total of 5×10^4 cells/well were seeded on the coating surfaces (φ 10 mm × 1 mm) in 24 well plate and cultured in 1 mL culture medium. After culturing for 3 days, the medium was replaced with 0.9 mL of culture medium and 0.1 mL of CCK-8 working solution for an additional culture duration of 3 h, with 100 μL of the reacted reagent extracted and transferred to a 96-well plate. Wells with identical concentrations CCK-8 working solution without cells were used as blank controls. Absorbance was measured using a microplate reader at 450 nm absorbance to reflect the number of viable cells per well. Cell viability was represented as the mean ± standard deviation (SD) of the absorbance obtained from five wells per group.

2.2.2. Cell Apoptosis Assay

Cellular apoptosis was determined using the Annexin V/FITC apoptosis detection kit (Beyotime, Nantong, China) conducted under flow cytometry. Briefly, MC3T3-E1 cells were seeded in a 6-well plate with a Ti-6Al-4V disk (φ 34 mm × 1 mm) coated with CeO_2 at a density of 2×10^5 cells/well. Cells cultured on 6-well plates with Ti-6Al-4V disks served as the control group. After culturing in 2 mL 10% FBS for 24 h, the cells were harvested by trypsinization and rinsed twice with PBS. The cell suspension was subsequently centrifuged at 1000 rpm for 3 min. Obtained cells were then resuspended in Annexin V and propidium iodide (PI) (BD Pharmingen, Franklin Lakes, NJ, USA) stain according to the manufacturer's instructions. Apoptotic cell fractions were analyzed by FACScan flow cytometry (Becton-Dickinson, San Jose, CA, USA). Early apoptotic cells (Q2: Annexin V+/PI− staining) and late apoptotic cells (Q4: Annexin V+/PI+ staining) were classified as undergoing apoptosis, with the proportion of these cells out of the total cell count was determined and presented.

2.2.3. Osteogenic Differentiation Assay

BMSCs cells with 2 mL culture medium were seeded on Ti-6Al-4V disks (φ 34 mm × 1 mm) with or without CeO_2 coating in 6-well plates at a density of 10^5 cells/well. After 24 h of incubation, the culture medium was replaced with equal volumes of osteoinduction medium. Cells seeded on Ti-6Al-4V disks without CeO_2 coating served as controls. The osteoinduction medium was composed of DMEM supplemented with 10% FBS, 1% antibiotics, 50 μg/mL ascorbic acid (Sigma, St Louis, MO, USA), 10 mmol/L sodium β-glycerophosphate (Sigma, St Louis, MO, USA), and 10 nmol/L dexamethasone (Sigma, St Louis, MO, USA). Quantitative real-time PCR (qPCR) was applied to test the expression of osteogenesis-associated genes including alkaline phosphatase (ALP), bone sialoprotein (BSP) and osteocalcin (OCN), with their respective primer sequences listed below. TRIzol reagent (Invitrogen, Carlsbad, CA, USA) was used to extract RNA at 0, 7, and 14 days. Then, the extracted RNA was

translated into cDNA with a PCR kit (Takara, Japan). Finally, qPCR was performed with an ABI 7500 Real-Time PCR system (Applied Biosystems, Waltham, MA, USA) as follows: Hot start at 95 °C for 5 min in the holding stage; 95 °C for 10 s and 60 °C for 30 s for 40 cycles in the cycling stage; and 95 °C for 15 s, 60 °C for 1 min, and 60 °C for 15 s in the melt curve stage. The PCR products were normalized to GAPDH, and relative gene expression was calculated using the $2^{-\Delta\Delta Ct}$ method. Each sample was examined in triplicate. Sequences for the primers used in qPCR are as listed in Table 1.

Table 1. Sequences for the primers used in qPCR.

ALP	forward	5′-GCC CTC TCC AAG ACA TAT A-3′
	reverse	5′-CCA TGA TCA CGA TAT CC-3′
Bsp	forward	5′-AGG ACT GCC GAA AGG AAG GTT A-3′
	reverse	5′-AGT AGC GTG GCC GGT ACT TAA A-3′
Ocn	forward	5′-AGG GAG GAT CAA GTC CCG-3′
	reverse	5′-GAA CAG ACT CCG GCG CTA-3′
GAPDH	forward	5′-GGG AAG CCC ATC ACC ATC TT-3
	reverse	5′-GGG AAG CCC ATC ACC ATC TT-3

Following 14 days of culturing in osteogenic induction, BMSCs in respective groups were lysed using a protein extraction kit (Piece, Rockford, IL, USA). Protein concentrations were determined using a bicinchoninic acid protein assay kit (Piece, Rockford, IL, USA) according to the manufacturer's protocols. Briefly, equal amounts of protein per sample (25 μg) were separated and transferred onto nitrocellulose membranes (Millipore Corporation, Billerica, MA, USA). After blocking with 5% skim milk, the primary antibodies of rabbit anti-mouse Smad 1 (1:1000, Bioworld Technology, Inc., St Louis Park, MN, USA), rabbit anti-mouse OCN (1:500, Abcam, Inc., Cambridge, MA, USA), and rabbit anti-mouse GAPDH (1:5000, Proteintech, Inc., Wuhan, China) were applied to each group. The membranes were subsequently washed three times and incubated with goat anti-rabbit IRDye 680 (1:10,000; Invitrogen, USA). After the final wash, the membranes were visualized using an Odyssey LI-CDR system, with representative images captured.

2.3. Antibacterial Effects of the CeO_2 Coating on Ti-6Al-4V Disks

2.3.1. Direct Contact (DCT) and CCK-8 Tests

E.f. ATCC 29,212 (American Type Culture Collection, Manassas, VA, USA), *P.g.* ATCC 33,277 and *P.i.* ATCC 25,611 were chosen for this study. The bacteria were grown overnight in 3% tryptic soy broth (TSB) (3 g of TSB powder in 100 g of water), at 37 °C in an anaerobic environment (80% N_2, 10% H_2 and 10% CO_2). The bacteria were subsequently suspended and diluted to 10^6 cells/mL in 3% TSB culture medium.

For antibacterial analysis, direct contact tests were conducted to analyze antimicrobial activity. In brief, diluted cell suspensions (0.5 mL, 1×10^6/mL) of *E.f.*, *P.g.*, and *P.i.* were seeded onto six Ti-6Al-4V disks (ø 10 mm × 1 mm) coated with CeO2 in 24-well plates. Identical cell suspensions seeded on Ti-6Al-4V disks without coating were used as negative controls; simultaneously, wells with TSB culture medium but without bacteria were used as blank controls. After 24 h incubation, the bacteria on the disks were collected and resuspended in 1 mL of 3% TSB culture medium. Five duplicates per group, each containing 100 uL of the above bacterial suspension, was transferred into in 96-well plates. The absorbance of each well was measured at 630 nm with a microplate reader (Bio-Tek, Winooski, VT, USA).

Bacterial proliferation was evaluated by a CCK-8 assay kit (Dojindo Molecular Technologies, Inc., Kumamoto, Japan) in accordance with the manufacturer's protocols. 200 uL *E.f.*, *P.g., and P.i.* cell suspension (1×10^6/mL) were seeded onto five CeO_2-coated Ti-6Al-4V disks per group

(ø 10 mm × 1 mm) placed in 24-well plates. Then, 100 µL of the above surplus diluted bacterial suspensions with 10 µL of CCK-8 was added to a 96-well plate for another 2 h of culture. Wells with CCK-8 solution but without bacteria were used as blank controls. The absorbance of each well was measured by using a microplate reader at 450 nm. Cell viability was represented as the mean ± standard deviation (SD) of the absorbance for five wells from each group.

2.3.2. Colony-Forming Unit Test (CFU)

Two hundred microliters *E.f.*, *P.g., and P.i.* cell suspension (1×10^6/mL) were seeded onto five CeO_2-coated Ti-6Al-4V disks per group (ø 34 mm × 1 mm). A film over the disk was used to help create contact and in an anaerobic environment. Ti-6Al-4V disks without coating were used as blanks. After 24 h culture, the microorganisms were subsequently removed from the samples and suspended in 1 mL of PBS in a cell culture dish. Twenty microliters of the above bacterial suspensions were then inoculated onto nutrient agar plates and cultured at 37 °C for 24 h. Colonies formed on the agar were viewed under light microscopy, with representative images captured and the number of cell colonies counted.

2.3.3. Live/dead Bacteria Staining

Antibacterial effects of the CeO_2 coating were further evaluated via live/dead staining. One hundred microliters of surplus *E.f.* bacteria suspended in PBS (from Section 2.3.2) were transferred to a culture plate and stained using a live/dead BacLight bacterial viability kit, in accordance with the manufacturer's instructions, and bacterial suspensions were chosen and imaged using confocal laser scanning microscopy (CLSM) (Carl Zeiss, Oberkochen, German) at excitation wavelengths of 488 nm (Calcein-AM) and 555 nm (propidium iodide). Then, the percent distribution of live and dead bacteria was analyzed according to the green and red fluorescence. Images were obtained with a 20× objective, and at least three images were collected randomly from each sample.

2.4. Statistical Analysis

All experiments were repeated thrice. Statistical analyses were conducted with using GraphPad Prism software, version 5.0 (GraphPad Software, Inc., La Jolla, CA, USA). Obtained results are expressed as the mean ± standard deviation (SD) and analyzed using one-way ANOVA with a post hoc test, with a p-value < 0.05 considered as statistically significant.

3. Results

3.1. Characterization of the CeO_2-Sprayed Coating

X-ray diffraction (XRD) patterns of the CeO_2 sprayed coating is used to infer its phase composition, with the results illustrated in Figure 1A. The coating was composed of the CeO_2 phase (JCPDS no. 34-0394) corresponding to the planes of (111, 200, 220, 311). The X-ray photoelectron spectra (XPS) of the CeO2 coating are shown in Figure 1B. The spectra revealed the presence of a mixed valence state (Ce^{3+} and Ce^{4+}) on the surface of the CeO_2-modified coating. For quantitative estimation of Ce^{3+} concentration in the CeO_2 coating, the ratio of Ce^{3+} in the total Ce content was calculated from the total areas under the Gaussian fitting peaks for each respective Ce^{3+} and Ce^{4+} state, using the equation for the ratio of peak areas reported in literature [26]; the percent of Ce^{4+} in the CeO_2 coating was calculated to be approximately 72.8%, indicating a major composition of Ce^{4+} valences present. SEM results shows the roughness of the CeO_2 coating in Figure 1C. The as-sprayed coating exhibited rough and uneven surfaces in the third electron image.

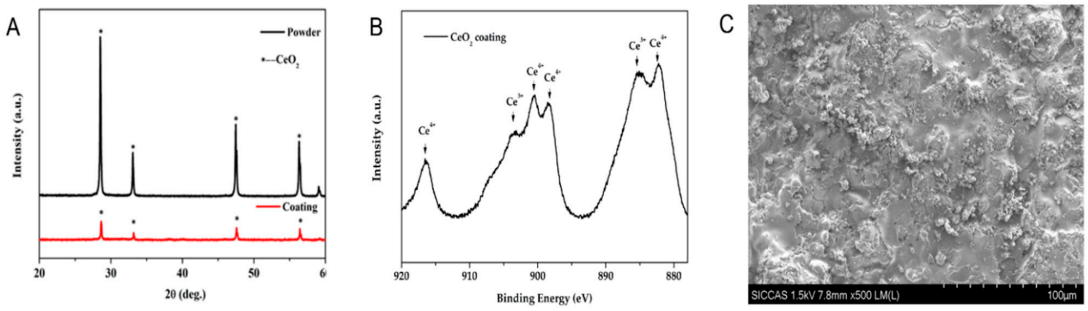

Figure 1. Structural and compositional characterization of the plasma-sprayed CeO_2 coating. (**A**) X-ray diffraction (XRD) patterns of the CeO_2 coating. Distribution of peaks were characteristic of CeO_2. (**B**) X-ray photoelectron spectroscopy spectra of the CeO_2 coating. The spectra revealed the presence of a mixed valence state (Ce^{3+} and Ce^{4+}) on the surface of the CeO_2 modified coatings, with Ce^{4+} accounting for 72.8% as calculated from the distribution ratio of their respective Gaussian fitting peaks. (**C**) SEM result revealed a rough texture present on the surface of the CeO_2 coating.

3.2. Biocompatibility of CeO_2 Coating

The biocompatibility of the CeO_2 coating in BMSCs and MC3T3-E1 cells was assessed by CCK-8 and cell apoptosis assays. CCK-8 results demonstrated no statistically significant difference in viability of BMSCs (Figure 2A) and MC3T3-E1 cells (Figure 2B) seeded on the CeO_2 coating, as compared to equivalent groups seeded on Ti-6Al-4V surface (#: $p > 0.05$). Similar results were observed from the flow cytometry analysis. Additionally, the percentage of apoptotic MC3T3-E1 cells (Q2 + Q4) seeded on the CeO_2 coating was statistically significantly lower than that on the Ti-6Al-4V surface (6.7% compared to 24.0%) as shown in Figure 2C. The above results indicated that the CeO_2 coating on the Ti-6Al-4V disks demonstrated good biocompatibility.

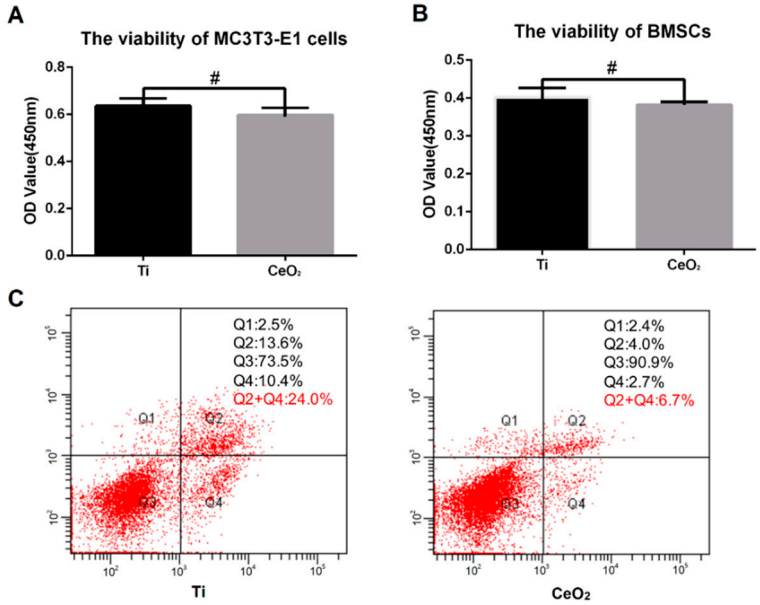

Figure 2. Biocompatibility of CeO_2 coating towards bone marrow stem cells (BMSCs) and MC3T3-E1 cells. (**A**,**B**) CCK-8 results demonstrated improved viability of BMSCs (**A**) and MC3T3-E1 cells (**B**) seeded on CeO2 coating after a 3-day culture period, as compared to uncoated Ti-6Al-4V surfaces (#: $p > 0.05$) ($n = 5$). (**C**) Flow cytometry analysis conducted on MC3T3-E1 cells cultured on CeO_2 coated Ti-6Al-4V surfaces. Percentage of apoptotic cells (Q2 + Q4) on the CeO_2 coating was measured at 6.7%, significantly lower than the percentage of apoptotic cells measured on the Ti-6Al-4V surface at 24.0% ($p < 0.05$) ($n = 3$).

3.3. Osteogenic Ability of the CeO_2 Coating

To directly address a functional role for the CeO_2 coating in osteogenic ability, the mRNA and protein expression of mineralization-related genes *ALP*, *Ocn*, and *Bsp* were measured after 7-day and 14-day BMSCs cell culture in osteoinduction medium. Compared with the control group, the CeO_2 coating significantly increased the mRNA levels of *ALP* (A), *Bsp* (B), and *Ocn* (C) ($p < 0.05$) at 7 and 14 days ($p < 0.01$), as shown in Figure 3A–C. Additionally, compared to groups cultivated on nontreated Ti-6Al-4V surface, the protein levels of OCN and Smad 1 were upregulated in the CeO_2 coating group at 14 days as shown in Figure 3D. These combined results indicate the ability of Ce^{4+}-rich CeO_2 coating in promoting osteogenesis in BMSCs.

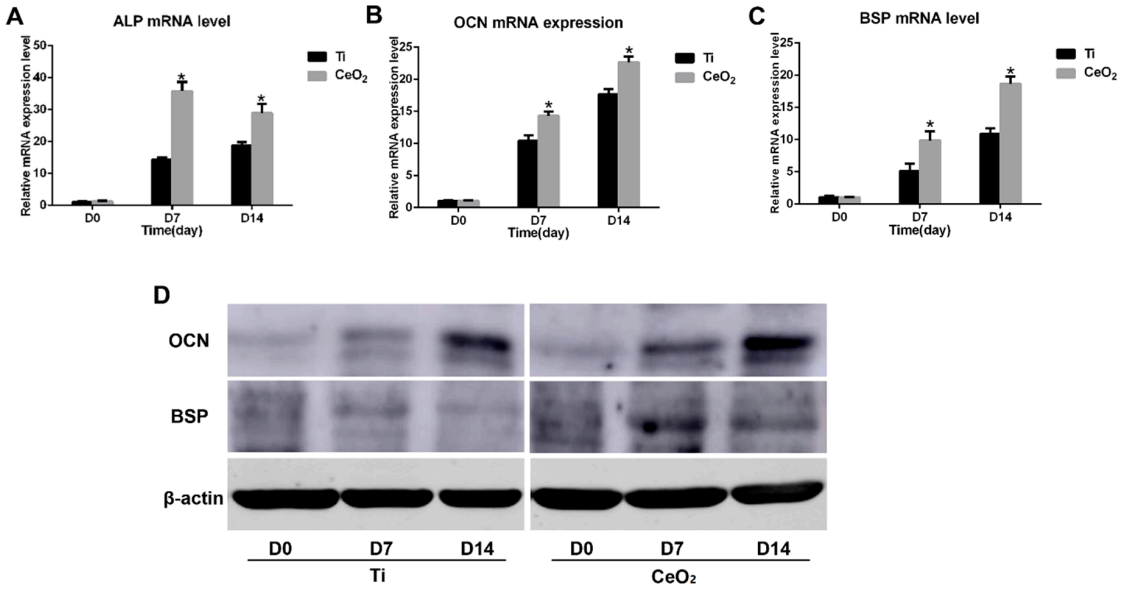

Figure 3. Osteogenic effect of CeO_2 coatings induced on BMSCs. (**A**–**C**) Expression levels of the osteogenic mRNA markers alkaline phosphatase (ALP), osteocalcin (OCN), and bone sialoprotein (BSP) at days 7 and 14 were significantly increased in CeO_2 groups as compared with uncoated Ti-6Al-4V control groups (*, $p < 0.05$;) ($n = 3$). (**D**) Western blot analysis of OCN, BSP, and β-actin protein expression levels level. Upregulation of both OCN and BSP of were observed in the CeO_2 coating group compared to the Ti-6Al-4V control group ($n = 3$).

3.4. Antibacterial Activity

E.f., *P.g.*, and *P.i.* viability on the CeO_2 coating was assessed by DCT and CCK-8 assays to ascertain the antibacterial effects of the CeO_2 coating. DCT (Figure 4A) and CCK-8 (Figure 4B) results indicate a significant decrease in viability of *E.f.*, *P.g.* and *P.i.* bacteria seeded on CeO_2 coating, as compared with corresponding groups seeded on pure Ti-6Al-4V discs. As shown in Figure 5, CFU results affirm similar findings with significantly lower bacterial viability on the CeO_2 coating compared to the respective control groups for *E.f.*, *P.g.*, and *P.i.* To further elucidate the antibacterial effects of the CeO_2 coating, live/dead staining of seeded *E.f.* bacteria (Figure 6A) show a significantly higher percent of dead bacteria (approximately 74.3%, stained in red) in the CeO_2 coating group, compared to the control group (approximately 4.1%) in Figure 6B. The combined results illustrate the antibacterial activity of the CeO_2 coating on the Ti-6Al-4V surface against *E.f.*, *P.g.*, and *P.i.*, which are the main pathogens involved in peri-implantitis.

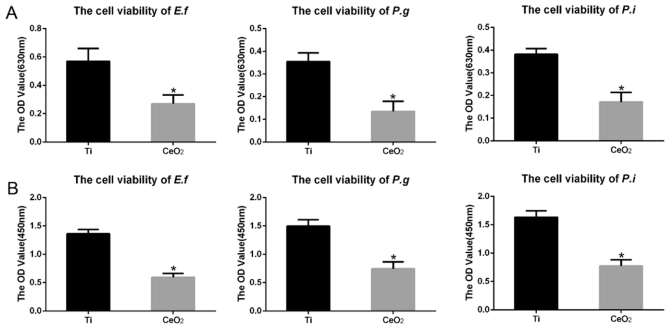

Figure 4. Viability of *E.f.*, *P.g.*, and *P.i.* seeded on CeO_2 coating. (**A**) DCT results indicate a significantly decreased viability of *E.f.*, *P.g.*, and *P.i.* on CeO_2 coatings as compared to the uncoated Ti-6Al-4V control group after 24 h culture. (**B**) CCK-8 results illustrate a similar trend of decreased viability among all CeO_2-coated groups after 24 h culture (*, $p < 0.05$;) ($n = 5$).

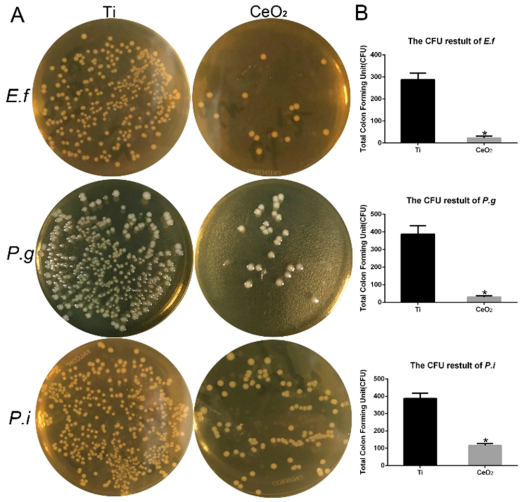

Figure 5. Colony-forming ability of *E.f.*, *P.g.*, and *P.i.* seeded on CeO_2 coating. (**A**) Observed under light microscopy, colony-forming unit (CFU) assays conducted after 24 h culture indicate a significant decrease in the number of *E.f.*, *P.g.*, and *P.i.* colonies on the CeO_2 coating as compared to the control group. (**B**) Statistical analysis indicates significantly reduced CFU numbers among all CeO_2 experimental groups. (*, $p < 0.05$;) ($n = 3$).

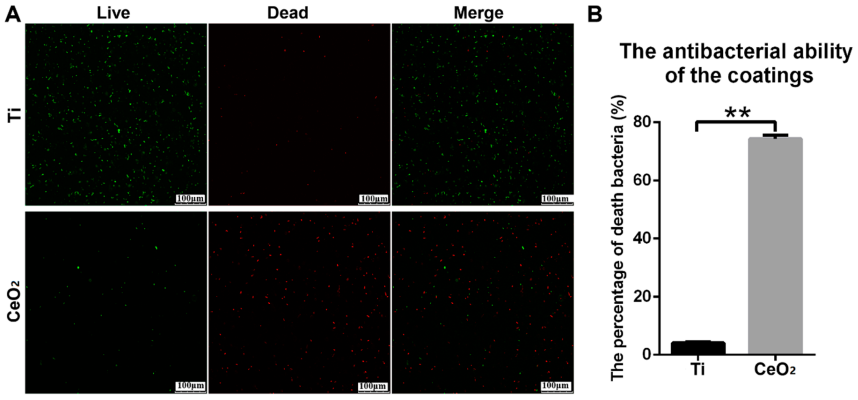

Figure 6. Live/dead staining of *E.f* seeded on CeO_2 coating. (**A**) Staining results of live *E.f* cells (staining with green) and dead *E.f* cells (staining with red) illustrate decreased viability in *E.f* cells seeded on CeO_2-coated Ti-6Al-4V discs. (**B**) Statistical analysis reveals the percentage of dead *E.f* cells was approximately 74.3% in the CeO_2-coated group, significantly higher than the percentage of dead E.f cells (4.1%) measured in the control group. (**, $p < 0.01$).

4. Discussion

Titanium and its alloys (most significantly grade 5 titanium alloy, Ti-6Al-4V) have favorable biocompatibility and mechanical properties, contributing to their widespread use as dental implants [2]. Correspondingly, the amount of bacterial colonization and the osteogenic ability of cells around the titanium alloy implants affect the final survival rate of dental implants [27]; prevention is the ideal method for implant-associated infection, with professional implant surface cleaning for bacterial adherence. Therefore, antibacterial surface coatings on dental implants have attracted great attention due to the development of their surface properties [28,29].

Amongst newly developed or adopted biomaterials, some have demonstrated strong antibacterial activity potentially useful for clinical usage or dental implant applications [30]; one of which is ceria (CeO_2). CeO_2 as a rare earth oxide has been gaining wide attention in various biomedical applications, such as anti-inflammatory and tissue regeneration applications, due to its free radical scavenging activity [31]. In our previous study, we found that incorporating CeO_2 into a calcium silicate coating enhances ALP activity and antibacterial activity [26]. The aim of our current study was to determine the osteogenic activity and antibacterial activity of a CeO_2 coating containing high Ce^{4+} valence proportion on a Ti-6Al-4V surface, with the express purpose of evaluating CeO_2-coated Ti-6Al-4V as a potential dental implant biomaterial.

As the use of CeO_2 coatings containing high proportions of Ce^{4+} valences on Ti-6Al-4V metal surfaces has yet to be reported, we first sought to classify and characterize our CeO_2 coating from a structural point of view. Both X-ray diffraction (Figure 1A) and X-ray photoelectron spectroscopy (Figure 1B) results verify the CeO_2 chemical composition and indicate the major contribution of Ce^{4+} over Ce^{3+} valences in the coating. The additional SEM images (Figure 1C) allows visualization of the microtexture present owing to the spray-coating process; the corresponding coarseness may help attachment of BMSCs and prove beneficial to the osteogenesis process critical to the survival rate of dental implants [2–4].

We then tested the osteogenic activity of the CeO_2 coating in vitro to optimize the mechanical performance of dental implants and to improve their survival rate. In our study, the CeO_2 coating demonstrated good biocompatibility on both BMSCs and MC3T3-E1 cells, as shown in Figure 2. Further evidence could be ascertained from the flow cytometry results, in which the percentage of apoptotic MC3T3-E1 cells (Q2 + Q4) seeded on the CeO_2 coating was statistically significantly lower than that on the Ti-6Al-4V surface (6.7% compared to 24.0%) as shown in Figure 2C. Additionally, the CeO_2 coating promoted the osteogenic ability of BMSCs with a corresponding significant increase in expression levels of all three selected osteogenesis gene markers (Figure 3A–C), along with a similar increase in protein expression (Figure 3D). This illustrates a similar trend as discovered in our previous study [24].

From an etiological point of view, an imbalance between the host response and bacteria is a significant contributing factor in inducing peri-implant disease, as observed in susceptible patients [32]. Because of the complex and varied oral consortium, it is extremely difficult to pinpoint a single or a group of microorganisms as the cause of peri-implant disease [33]. We chose *E.f.*, *P.g.*, and *P.i.* as representative targets in identifying the antibacterial activity of our coating. *E.f.*, *P.g.*, and *P.i.* are oral pathogens that are difficult to eliminate, and have been implicated to play at least a significant role in developing periodontitis or peri-implantitis [34], with further evidence highlighting their roles in individuals with chronic and refractory periodontitis [35,36]. Correspondingly, our results indicate the antibacterial activity of the CeO_2 coating against *E.f.*, *P.g.*, and *P.i.* in vitro. The proliferation and viability of *E.f.*, *P.g.*, and *P.i.* were significantly inhibited after CeO_2 coating compared with the Ti-6Al-4V surface alone by the DCT (Figure 4A) and CCK-8 (Figure 4B) assays. CFU and live/dead bacterial staining were further used to detect bacterial viability. Both results showed that the bacterial viabilities of *E.f.*, *P.g.*, and *P.i.* on the CeO_2 coating were significantly lower than that of the control groups, demonstrating that the CeO_2 coating has the ability to impact the survivability of *E.f.*, *P.g.*, and *P.i.*, which are major pathogens involved in peri-implantitis. Both the inflammation and source of pathogens (e.g., *E.f.*, *P.g.*, and *P.i.*) observed in peri-implantitis result in reactive oxygen species (ROS)

production; Selvaraj et al. reported that CeO_2 decreased cellular ROS production, which inhibited proinflammatory mediator expression by attenuating the activity of NF-κB [37]. Scavenging of free radicals is a way of eliminating ROS production and reducing the inflammatory response; CeO_2 coating with a high level of Ce^{4+} on the surface was demonstrated to possess catalase mimetic activity, which could breakdown H_2O_2 into molecular oxygen and therefore scavenge free radicals present from ROS production. This may be a major mechanism achieved by the Ce^{4+}-containing CeO_2 coating in our study.

Despite having discovered significant results on the antimicrobial and osteogenic activity of our CeO_2 coating, there are certain limitations of our study that could possibly be further addressed to ascertain the suitability of CeO_2-coated titanium as a dental implant biomaterial. The first of which would direct towards the absence of in vivo biocompatibility results to determine whether CeO_2-coated Ti-6Al-4V elicits significant immune response; despite the novel combination of the two materials in a dental clinical usage setting, both CeO_2 and Ti-6Al-4V have previously been reported in the literature to possess positive biocompatibility in vivo [38–40]. Henceforth, we believe the physical combination of CeO_2 and Ti-6Al-4V as observed in our study to possess a low risk of inciting significant immune response; this could be a possible investigation area for a future study. Additionally, owing to the complex interactions between various cell types in the oral cavity, it would have been a closer reflection of the oral cavity if BMSCs and/or MC3T3-E1 cells were co-cultured with other cell types (such as oral mucosal epithelial cells and oral keratinocytes) in our experiments. However, owing to the focus of our study being the antimicrobial activity of CeO_2 coating towards oral microbiota and its osteogenic activity elicited towards BMSCs/MC3T3-E1 cells, it may have been an unnecessary complication to co-culture with further oral cell types as they are not directly involved in CeO_2 activity and may potentially confound results.

5. Conclusions

In this study, plasma-sprayed CeO_2 coating on Ti-6Al-4V surfaces with high composition of Ce^{4+} valences significantly enhanced antibacterial activity towards oral microbiota, along with increased osteogenic activity in BMSCs and MC3T3-E1 cells. These results illustrate the potential of CeO_2-coated Ti-6Al-4V constructs in dental implant applications, to reduce the occurrence of peri-implantitis and implant failures as induced by oral microbiota.

Author Contributions: J.Y. and Y.X. conceived and designed the experiments, S.Q., Z.J. and H.L. performed the experiments, J.Y., G.S. and F.C. acquired and analysed the data, J.Y.Z.J. and S.Q. wrote the manuscript, D.W. and H.L.E.P. revised the manuscript. All authors have read and agreed to the published version of the manuscript.

Funding: This work was funded by the Natural Science Foundation of Shanghai (grant no. 19ZR1439600).

Conflicts of Interest: The authors claim to have no financial interest, either directly or indirectly, in the products or information listed in the article.

References

1. Smeets, R.; Henningsen, A.; Jung, O.; Heiland, M.; Hammaecher, C.; Stein, J.M. Definition, etiology, prevention and treatment of peri-implantitis—A review. *Head Face Med.* **2014**, *10*, 34. [CrossRef]
2. Tenenbaum, H.; Bogen, O.; Séverac, F.; Elkaim, R.; Davideau, J.L.; Huck, O. Long-term prospective cohort study on dental implants: Clinical and microbiological parameters. *Clin. Oral. Implant. Res.* **2017**, *28*, 86–94. [CrossRef] [PubMed]
3. Norowski, P.A.; Bumgardner, J.D. Biomaterial and antibiotic strategies for peri-implantitis: A review. *J. Biomed. Mater. Res. B Appl. Biomater.* **2009**, *88*, 530–543. [CrossRef] [PubMed]
4. Leonhardt, Å.; Renvert, S.; Dahlén, G. Microbial findings at failing implants. *Clin. Oral. Implant. Res.* **1999**, *10*, 339–345. [CrossRef] [PubMed]
5. Zhuang, L.F.; Watt, R.M.; Mattheos, N.; Si, M.S.; Lai, H.C.; Lang, N.P. Periodontal and peri-implant microbiota in patients with healthy and inflamed periodontal and peri-implant tissues. *Clin. Oral. Implant. Res.* **2016**, *27*, 13–21. [CrossRef] [PubMed]

6. Cardoso, M.; Sangalli, J.; Koga-Ito, C.Y.; Ferreira, L.L.; da Silva Sobrinho, A.S.; Nogueira, L. Abutment Coating with Diamond-Like Carbon Films to Reduce Implant—Abutment Bacterial Leakage. *J. Periodontol.* **2016**, *87*, 168–174. [CrossRef]
7. Chatzistavrou, X.; Fenno, J.C.; Faulk, D.; Badylak, S.; Kasuga, T.; Boccaccini, A.R.; Papagerakis, P. Fabrication and characterization of bioactive and antibacterial composites for dental applications. *Acta Biomater.* **2014**, *10*, 3723–3732. [CrossRef]
8. Razavian, H.; Barekatain, B.; Shadmehr, E.; Khatami, M.; Bagheri, F.; Heidari, F. Bacterial leakage in root canals filled with resin-based and mineral trioxide aggregate-based sealers. *Dent. Res. J. Isfahan* **2014**, *11*, 599–603.
9. Kirmanidou, Y.; Sidira, M.; Drosou, M.-E.; Bennani, V.; Bakopoulou, A.; Tsouknidas, A.; Michailidis, N.; Michalakis, K. New Ti-Alloys and Surface Modifications to Improve the Mechanical Properties and the Biological Response to Orthopedic and Dental Implants: A Review. *Biomed Res. Int.* **2016**, *2016*, 1–21. [CrossRef]
10. Romeo, E.; Ghisolfi, M.; Murgolo, N.; Chiapasco, M.; Lops, D.; Vogel, G. Therapy of peri-implantitis with resective surgery. A 3-year clinical trial on rough screw-shaped oral implants. Part I: Clinical outcome. *Clin. Oral. Implant. Res.* **2005**, *16*, 9–18. [CrossRef]
11. Elias, C.N.; Lima, J.H.C.; Valiev, R.; Meyers, M.A. Biomedical applications of titanium and its alloys. *JOM* **2008**, *60*, 46–49. [CrossRef]
12. Li, K.; Yu, J.; Xie, Y.; Huang, L.; Ye, X.; Zheng, X. Effects of Zn content on crystal structure, cytocompatibility, antibacterial activity, and chemical stability in Zn-modified calcium silicate coatings. *J. Therm. Spray Technol.* **2013**, *22*, 965–973. [CrossRef]
13. Romeo, E.; Lops, D.; Chiapasco, M.; Ghisolfi, M.; Vogel, G. Therapy of peri-implantitis with resective surgery. A 3-year clinical trial on rough screw-shaped oral implants. Part II: Radiographic outcome. *Clin. Oral. Implant. Res.* **2007**, *18*, 179–187. [CrossRef]
14. Serino, G.; Turri, A. Outcome of surgical treatment of peri-implantitis: Results from a 2-year prospective clinical study in humans. *Clin. Oral. Implant. Res.* **2011**, *22*, 1214–1220. [CrossRef] [PubMed]
15. Thierbach, R.; Eger, T. Clinical outcome of a nonsurgical and surgical treatment protocol in different types of peri-implantitis: A case series. *Quintessence Int.* **2013**, *44*, 137–148.
16. Roccuzzo, M.; Bonino, F.; Bonino, L.; Dalmasso, P. Surgical therapy of peri-implantitis lesions by means of a bovine-derived xenograft: Comparative results of a prospective study on two different implant surfaces. *J. Clin. Periodontol.* **2011**, *38*, 738–745. [CrossRef]
17. Kaluđerović, M.R.; Schreckenbach, J.P.; Graf, H.L. Titanium dental implant surfaces obtained by anodic spark deposition—From the past to the future. *Mater. Sci. Eng. C* **2016**, *69*, 1429–1441. [CrossRef]
18. Li, K.; Xie, Y.; Ao, H.; Huang, L.; Ji, H.; Zheng, X. The enhanced bactericidal effect of plasma sprayed zinc-modified calcium silicate coating by the addition of silver. *Ceram. Int.* **2013**, *39*, 7895–7902. [CrossRef]
19. Li, K.; Liu, S.; Hu, T.; Razanau, I.; Wu, X.; Ao, H.; Huang, L.; Xie, Y.; Zheng, X. Optimized Nanointerface Engineering of Micro/Nanostructured Titanium Implants to Enhance Cell–Nanotopography Interactions and Osseointegration. *ACS Biomater. Sci. Eng.* **2020**, *6*, 969–983. [CrossRef]
20. Thill, A.; Zeyons, O.; Spalla, O.; Chauvat, F.; Rose, J.; Auffan, M.; Flank, A.M. Cytotoxicity of CeO2 Nanoparticles for Escherichia coli. Physico-Chemical Insight of the Cytotoxicity Mechanism. *Environ. Sci. Technol.* **2006**, *40*, 6151–6156. [CrossRef]
21. Li, K.; Hu, D.; Xie, Y.; Huang, L.; Zheng, X. Sr-doped nanowire modification of Ca–Si-based coatings for improved osteogenic activities and reduced inflammatory reactions. *Nanotechnology* **2018**, *29*, 84001. [CrossRef] [PubMed]
22. Hu, D.; Li, K.; Xie, Y.; Pan, H.; Zhao, J.; Huang, L.; Zheng, X. Different response of osteoblastic cells to Mg 2+, Zn 2+ and Sr 2+ doped calcium silicate coatings. *J. Mater. Sci. Mater. Med.* **2016**, *27*, 56. [CrossRef] [PubMed]
23. Li, K.; Shen, Q.; Xie, Y.; You, M.; Huang, L.; Zheng, X. Incorporation of cerium oxide into hydroxyapatite coating regulates osteogenic activity of mesenchymal stem cell and macrophage polarization. *J. Biomater. Appl.* **2017**, *31*, 1062–1076. [CrossRef]
24. You, M.; Li, K.; Xie, Y.; Huang, L.; Zheng, X. The Effects of Cerium Valence States at Cerium Oxide Coatings on the Responses of Bone Mesenchymal Stem Cells and Macrophages. *Biol. Trace Elem. Res.* **2017**, *179*, 259–270. [CrossRef] [PubMed]

25. Li, K.; Xie, Y.; You, M.; Huang, L.; Zheng, X. Plasma sprayed cerium oxide coating inhibits H_2O_2-induced oxidative stress and supports cell viability. *J. Mater. Sci. Mater. Med.* **2016**, *27*, 100. [CrossRef]
26. Li, K.; Yu, J.; Xie, Y.; You, M.; Huang, L.; Zheng, X. The Effects of Cerium Oxide Incorporation in Calcium Silicate Coating on Bone Mesenchymal Stem Cell and Macrophage Responses. *Biol. Trace Elem. Res.* **2017**, *177*, 148–158. [CrossRef] [PubMed]
27. Zhou, X.; Hu, X.; Lin, Y. Coating of Sandblasted and Acid-Etched Dental Implants With Tantalum Using Vacuum Plasma Spraying. *Implant Dent.* **2018**, *27*, 202–208. [CrossRef]
28. Chouirfa, H.; Bouloussa, H.; Migonney, V.; Falentin-Daudré, C. Review of titanium surface modification techniques and coatings for antibacterial applications. *Acta Biomater.* **2019**, *83*, 37–54. [CrossRef]
29. Mehdikhani-Nahrkhalaji, M.; Fathi, M.H.; Mortazavi, V.; Mousavi, S.B.; Hashemi-Beni, B.; Razavi, S.M. Novel nanocomposite coating for dental implant applications in vitro and in vivo evaluation. *J. Mater. Sci. Mater. Med.* **2012**, *23*, 485–495. [CrossRef]
30. Maria Magdalane, C.; Kaviyarasu, K.; Raja, A.; Arularasu, M.V.; Mola, G.T.; Isaev, A.B.; Al-Dhabi, N.A.; Arasu, M.V.; Jeyaraj, B.; Kennedy, J.; et al. Photocatalytic decomposition effect of erbium doped cerium oxide nanostructures driven by visible light irradiation: Investigation of cytotoxicity, antibacterial growth inhibition using catalyst. *J. Photochem. Photobiol. B Biol.* **2018**, *185*, 275–282. [CrossRef]
31. Estevez, A.Y.; Pritchard, S.; Harper, K.; Aston, J.W.; Lynch, A.; Lucky, J.J.; Ludington, J.S.; Chatani, P.; Mosenthal, W.P.; Leiter, J.C.; et al. Neuroprotective mechanisms of cerium oxide nanoparticles in a mouse hippocampal brain slice model of ischemia. *Free Radic. Biol. Med.* **2011**, *51*, 1155–1163. [CrossRef] [PubMed]
32. Mombelli, A.; Décaillet, F. The characteristics of biofilms in peri-implant disease. *J. Clin. Periodontol.* **2011**, *38*, 203–213. [CrossRef] [PubMed]
33. Belibasakis, G.N. Microbiological and immuno-pathological aspects of peri-implant diseases. *Arch. Oral Biol.* **2014**, *59*, 66–72. [CrossRef] [PubMed]
34. Canullo, L.; Orlato Rossetti, P.H.; Penarrocha, D. Identification of Enterococcus Faecalis and Pseudomonas Aeruginosa on and in Implants in Individuals with Peri-implant Disease: A Cross-Sectional Study. *Int. J. Oral Maxillofac. Implant.* **2015**, *30*, 583–587. [CrossRef]
35. Rams, T.E.; Feik, D.; Mortensen, J.E.; Degener, J.E.; van Winkelhoff, A.J. Antibiotic Susceptibility of Periodontal Enterococcus faecalis. *J. Periodontol.* **2013**, *84*, 1026–1033. [CrossRef]
36. Sun, J.; Sundsfjord, A.; Song, X. Enterococcus faecalis from patients with chronic periodontitis: Virulence and antimicrobial resistance traits and determinants. *Eur. J. Clin. Microbiol. Infect. Dis.* **2012**, *31*, 267–272. [CrossRef]
37. Selvaraj, V.; Manne, N.D.; Arvapalli, R.; Rice, K.M.; Nandyala, G.; Fankenhanel, E.; Blough, E.R. Effect of cerium oxide nanoparticles on sepsis induced mortality and NF-κB signaling in cultured macrophages. *Nanomedicine* **2015**, *10*, 1275–1288. [CrossRef]
38. Varini, E.; Sánchez-Salcedo, S.; Malavasi, G.; Lusvardi, G.; Vallet-Regí, M.; Salinas, A.J. Cerium (III) and (IV) containing mesoporous glasses/alginate beads for bone regeneration: Bioactivity, biocompatibility and reactive oxygen species activity. *Mater. Sci. Eng. C* **2019**, *105*, 109971. [CrossRef]
39. Strobel, C.; Förster, M.; Hilger, I. Biocompatibility of cerium dioxide and silicon dioxide nanoparticles with endothelial cells. *Beilstein J. Nanotechnol.* **2014**, *5*, 1795–1807. [CrossRef]
40. Haslauer, C.M.; Springer, J.C.; Harrysson, O.L.A.; Loboa, E.G.; Monteiro-Riviere, N.A.; Marcellin-Little, D.J. In vitro biocompatibility of titanium alloy discs made using direct metal fabrication. *Med. Eng. Phys.* **2010**, *32*, 645–652. [CrossRef]